applied sciences

MDPI

Article

Bulletproof Performance of Composite Plate Fabricated Using Shear Thickening Fluid and Natural Fiber Paper

Hyeonho Cho †, Jongsuk Lee †, Sungjin Hong and Sunghan Kim *

School of Mechanical Engineering, Chung-Ang University, Seoul 06974, Korea; ckror93@gmail.com (H.C.); wjrk2010@gmail.com (J.L.); hongluck36@gmail.com (S.H.)

* Correspondence: sunghankim@cau.ac.kr; Tel.: +82-2-820-5265

† Hyeonho Cho and Jongsuk Lee contributed equally to this work.

Received: 15 November 2019; Accepted: 17 December 2019; Published: 20 December 2019

Abstract: In the munitions industry, there have been considerable efforts spent to develop low-cost, simply fabricated, easily wearable, and biocompatible bulletproof armors. Recently, long fiber-reinforced composites and shear thickening fluids (STFs) were inceptively utilized to improve bulletproof performance with solid or fabric materials. In this study, Hanji, a cornstarch suspension, Korean traditional long fiber paper, and a well-known STF, respectively, were examined for bulletproof applications to evaluate their own effects on bulletproof performance; tests were carried out in the field and finite element analysis (FEA) was performed to evaluate the behavior of materials regarding with perforated clay areas from in-field tests. It was found that both Hanji and STF influenced the bullet penetration by two factors, namely the momentum of bullet and stress propagation. The cornstarch suspension, rather than Hanji, showed outstanding performance in decreasing the linear velocity of the bullet and minimized the stress propagation to the protecting object. Thus, although STF performed a key role in bulletproof performance, Hanji also proved to be a suitable material as an exterior covering for absorbing the initial impact stress and maintaining the durability and stability of the armor itself.

Keywords: bulletproof armor; Hanji; cornstarch suspension; shear thickening fluid; finite element analysis (FEA)

1. Introduction

Bulletproof armors are being developed to protect humans from destructive weapons. In particular, immense efforts are being directed toward developing low-cost, simply fabricated, easily wearable, and biocompatible bulletproof armors [1–7]. For example, Lee et al. developed a Kevlar fabric that was impregnated with a colloidal shear thickening fluid (STF) for improving the bulletproof performance of bulletproof materials compared to that of materials based only on Kevlar fabrics [4]. Shim et al. engineered composites composed of glass and a polymer for use as bulletproof materials through the strengthened-glass fabrication method [5]. Xie et al. fabricated nacre-mimetic bulletproof materials utilizing graphene oxide and silk fibroin with favorable flexibility [6]. However, these previous studies could not develop bulletproof materials satisfying all the requirements, namely low cost, simple fabrication process, easy wearability, and biocompatibility. In particular, the popular bulletproof materials such as Kevlar or aramid fibers are expensive; thus, further studies are needed to fabricate cost-effective bulletproof armors using facile fabrication methods.

Hanji, Korean traditional paper, is conventionally manufactured from natural cellulose fibers of mulberry trees. This paper is known as one of the strongest papers worldwide owing to its long fibers [8,9].

In addition, the paper has many advantages such as extraordinary flexibility, air permeability, humidity controllability, and biocompatibility; these properties have attracted the attention of researchers, resulting in its applications in several fields such as flexible electronics and packing papers [8,10]. Moreover, studies have focused on improving the mechanical properties of Hanji and developing its industrial mass production [11–13]. In particular, Hanji paper can be a potential candidate for bulletproof armors owing to its durability, stability, biocompatibility, and flexibility.

Non-Newtonian fluids can be potential materials for fabricating bulletproof armors owing to their fluidic dynamic behavior along with high shear rates. It has been reported that some colloidal suspensions have versatile viscosity with different shear rates, i.e., the so-called (STFs) and shear thinning fluids, in contrast to Newtonian fluids [14,15]. It is important for a flowing STF to show impact-generated solidification [16]. Many researchers have demonstrated that the shear thickening behavior causing solidification under impact forces or high shear rates is due to the self-organization of colloidal particles, the so-called impact-generated jamming and hydroclustering mechanism [16–19]. Furthermore, the self-organization of colloidal particles gives rise to significant energy dissipation [16,18]. Cornstarch colloidal suspensions are representative STF materials and have advantages such as extraordinary energy dissipation under impact or high shear forces. In particular, the cornstarch, which are low-cost and biocompatible materials, are easily dissolved in water to prepare cornstarch suspensions in facile way, and can thus be considered for developing bulletproof materials [20–22].

Therefore, in the present study, we fabricated cost-effective bulletproof biocomposites composed of natural fibers and cornstarch, which could be easily supplied everywhere. Furthermore, bulletproof performances for biocomposites were explored via bulletproof experiment and finite element analysis (FEA) simulation. The biocomposites were fabricated with cornstarch suspension (STF) layers and Hanji sheets through layer-by-layer (LbL) assembly, and witness clay pieces were adhered to the backside of all the fabricated bulletproof plates for evaluating their bulletproof properties. Various models with layers of different thicknesses were manufactured for analyzing the effect of cornstarch suspension and Hanji on bulletproof properties. Results showed that these hybrid composites comprising both Hanji and cornstarch suspension layers showed better ballistic protection performance compared to that of the composites composed of only Hanji, owing to the hydroclustering mechanism. The bulletproof performance of materials under impact loading could be analyzed by FEA simulation [23]. To determine the impact resistance of the developed bulletproof plate, the rapidly decreasing trend of the linear velocity in the cornstarch suspension layer and Hanji plate was analyzed via FEA. Moreover, the overall bulletproof performance was evaluated through a comparison of the experimental and simulation results. Many previous results showed that Kevlar fabrics, long fiber-reinforced composites, and composite STF were possessed superior bulletproof characteristics in terms of bullet resistance behavior [24,25]. This present study has focused on identifying the contribution of cornstarch STF and Hanji to the bullet resistance characteristics using two factors, namely the momentum of bullet and stress propagation. The findings of this study are beneficial for developing wearable, cost-effective, and large-scale bulletproof biocomposites composed of natural fibers and STFs through a facile fabrication approach.

2. Materials and Methods

2.1. Preparation of Bulletproof Plate Comprising Hanji and Cornstarch Suspensions

The composite plates were fabricated using the LbL method [26,27]. First, Hanji was assembled layer by layer using a water glue adhesive (Figure S1a). Second, the cornstarch suspension (55 wt %) was carefully prepared by blending cornstarch powder and water in the plastic basket, while steering the suspension with glove hands at room temperature, until the cornstarch completely dissolved in water. Third, the suspension was sealed twice: first in a zipper bag (inner) and then in a plastic airtight container (outer) (Figure S1b). Finally, the Hanji and cornstarch suspension layers were assembled

with adhesive tape, with the Hanji layer on the front side and cornstarch suspension layer on the back side (Figure S1c). During the fabrication process, different numbers of Hanji layers and various thicknesses of the cornstarch suspension layers were used, as mentioned in Table 1. To evaluate the performance of the fabricated bulletproof plates, a piece of witness clay was attached at the back of each composite plate with dimensions of 10 cm × 12 cm × 2 cm.

Table 1. Types of composite plates fabricated.

Type	Thickness of Cornstarch Suspensions (mm)	Number of Hanji Sheets
A	0	60
B	0	120
C	0	180
D	10	60
E	20	60
F	30	60

2.2. Bulletproof Experiment to Evaluate Performance in the Field

The performance of the bulletproof composites (around 15 cm × 20 cm) was evaluated in the field. A Glock 17 (handgun) with a 9-mm lead bullet was fired at the bulletproof composites from a distance of approximately 10 m. We analyzed the bulletproof performance based on the diameter of the clay piece after the bullet penetrated the plate.

2.3. FEA Simulation Methodology

FEA simulations were conducted to examine the bulletproof capacity of the composite plates using ABAQUS/CAE® software. Considering the high momentum during bullet impact, models were developed using the Explicit Dynamics step in the software with a total time period of 300 μs. To simulate actual field conditions, the bullet was designed to resemble a 9-mm lead bullet commercially used in the arms industry (Figure S2). It was set to behave as a discrete rigid body impacting the composite plate with a linear velocity of 407 m/s and rotational speed of 27,000 rpm. The composite plate was modeled to have an area 10 cm × 10 cm with variable thicknesses. The mechanical properties of Hanji and cornstarch suspension were obtained from previous studies [28,29].

3. Results and Discussion

3.1. Bulletproof Performance of the Different Composite Plates

To test the bulletproof performance of the fabricated composite plates, bullets were fired from a distance of 10 m. After the bullets penetrated the composite plates, the witness clay pieces, which were bonded on the backside of the plates, were perforated (Figure 1). Therefore, the perforated area of the witness clay piece, α, and initial bullet projection area, β, were determined. The perforated area was calculated from the perforated hole diameter (witness clay diameter), D, using the following popular formula:

$$\alpha = \pi D^2/4. \quad (1)$$

Moreover, the initial bullet projection area was the same as the bullet cross-section area, which could be easily obtained from the 9-mm diameter of bullet. Using these area values (α and β), the normalized perforated area, U, was calculated as follows:

$$U = \alpha/\beta. \quad (2)$$

The normalized perforated area (U) is an important parameter for evaluating bulletproof performance. For example, if the normalized perforated area is small, the overall bulletproof performance of the composite is considered satisfactory.

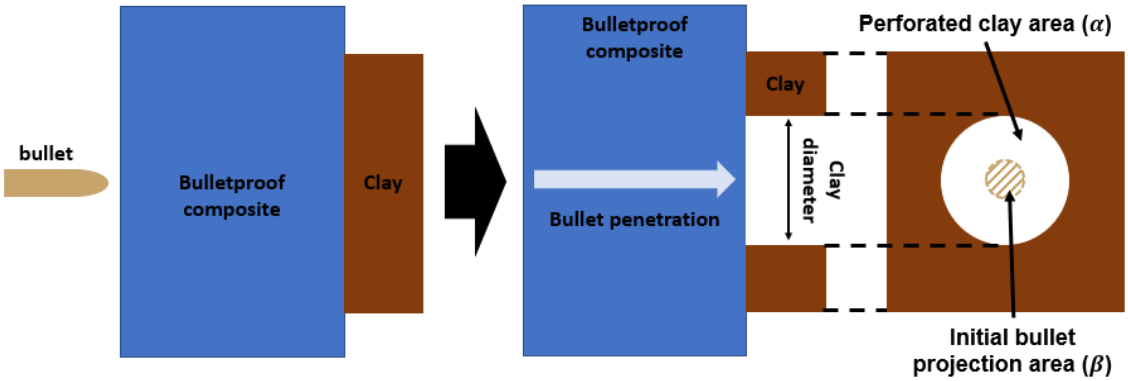

Figure 1. Schematic representation of the bullet penetrating the composite plate composed of Hanji and shear thickening fluids (STF) layers and clay perforation (clay diameter). The perforated witness clay area (α) and initial bullet projection area (β) were measured to calculate the normalized perforated area (U).

The normalized perforated area of the composites was analyzed for evaluating the bulletproof performance of the composites (Figure 2a,b). To evaluate the bulletproof performance of only Hanji layers without the cornstarch layers, the bulletproof experiment was conducted for composites composed of Hanji layers of different thicknesses without the cornstarch layers. Results showed that the normalized perforated area of the composites with different numbers of Hanji layers (60, 120, and 180 layers) gradually increased to 11.1, 47.3, and 75.5, respectively (Figure 2a). Furthermore, to analyze the influence of STF layers on the bulletproof performance of these composites, the bulletproof experiment was conducted for composites comprising Hanji layers and cornstarch suspension layers (Figure 2b). The normalized perforated area for the composites with a constant number of Hanji layers (60 layers) and different thicknesses of the cornstarch suspension layers (10, 20, and 30 mm) continuously reduced from 35.3 to 8.5 and then 3.9, respectively. Furthermore, (Figure 2a) the relationship between normalized perforated area, Y, and number of Hanji sheets, X, was expressed as:

$$Y = 0.54\,X - 19.87. \quad (3)$$

Moreover, the relationship between normalized perforated area and STF thickness, Z, was expressed as:

$$Y = -1.57\,Z + 47.30. \quad (4)$$

Throughout the relationships between the normalized penetrated area and the thickness of materials, the STF had a negative gradient on this relationship. Theoretically, the STF had the transition on its own state from liquid to solid under a high shear rate. This phenomenon contributed to the hydroclustered effect from the jamming of colloidal particles in STF. Thus, the resistance to the momentum of bullet was reinforced with this effect, and the normalized perforated area was decreased with increase of STF thickness. Figure S3 shows the actual perforated witness clay images obtained during the bulletproof experiments for the composite without cornstarch layers and having 120 Hanji layers along with that for the composite with a 20-mm-thick cornstarch suspension layer and 60 Hanji layers (Figure S3). In addition, the witness clay diameters for all composites were measured to calculate the normalized perforated area (Figure S4).

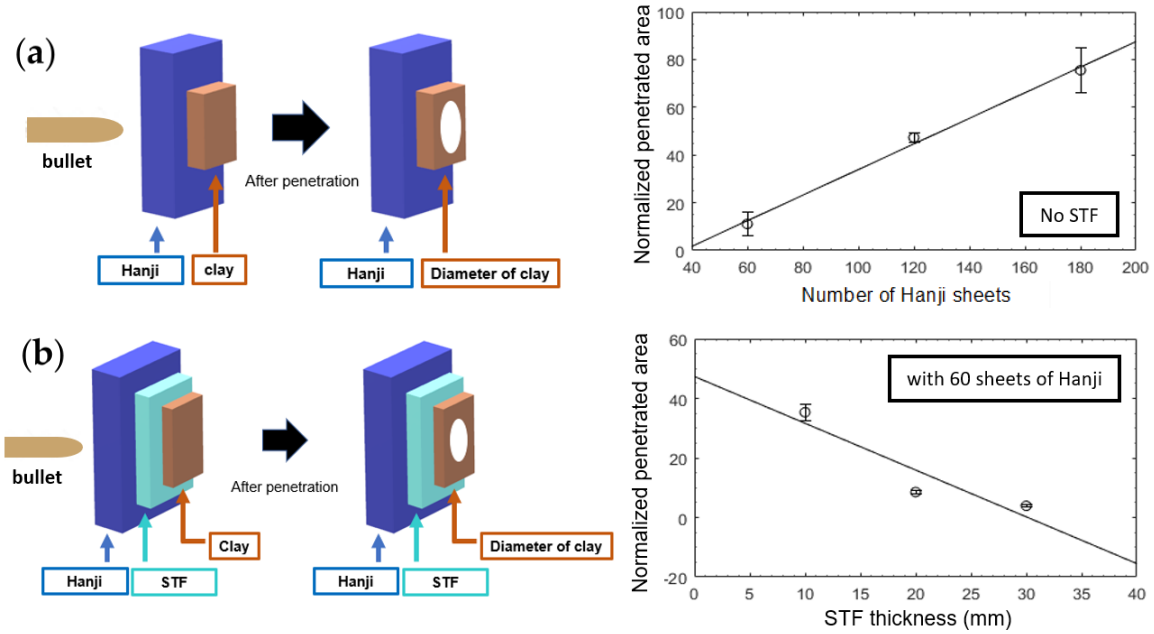

Figure 2. Schematics depicting the bulletproof experiments for (**a**) composites with only Hanji layers and (**b**) hybrid composites composed of Hanji and cornstarch suspension (STF) layers. The respective normalized penetrated areas are also presented in the graphs.

3.2. FEA Simulation for Evaluating the Dynamics of Hanji and Cornstarch in Response to Bullet Impact

The effects of Hanji and cornstarch suspension layers on the bullet velocity were estimated via FEA simulations. The mechanical properties of these materials are provided in Table S1, as obtained from previous studies [25,26]. We specifically assumed the cornstarch suspension to exhibit solid-like behavior under high shear rates during bullet impact [18]. Fall et al. researched the rheological behavior of cornstarch suspensions and estimated the complex shear modulus and yield stress in the solidified region [25,26]. These values were converted into properties of elasticity using the appropriate Poisson's ratio of 0.3. To establish the failure criteria, predefined shear failure values obtained from mechanical properties, namely the ultimate strength points of materials, were used by comparing the equivalent plastic strain (PEEQ) calculated through the built-in function in ABAQUS/CAE (see supporting information) [30]. For the composite plate, the sealing of the cornstarch suspension, which was used in the bulletproof test, was neglected to estimate only the performance of composite materials. The boundary conditions were set with the sides of the composite plate being fixed in all directions.

During the initial simulations performed with plates comprising 15-mm-thick Hanji and 30-mm-thick cornstarch suspension layers, the bullet penetrated the composite plates (Figure 3). During the penetration bullet, Hanji absorbed most of the impact stress rather than the cornstarch suspension. This difference in stress absorption between these materials was attributed to the superior elastic properties of Hanji. However, in the case of the perforated hole size, the cornstarch suspension layer had much larger holes than Hanji. The impact stress of the bullet after penetrating the Hanji layer was still high enough to cause failure of the cornstarch suspension layer. The suspension showed more plastic deformation at failure, despite having a low elastic modulus and strength. Thus, FEA simulations indicated the different failure modes of the materials caused by the bullet impact. From this difference in the failure modes between these materials, we anticipated that each layer of these materials would resist the bullet impact through different mechanisms. To analyze these mechanisms, the momentum of bullets was investigated in terms of changing the linear and angular velocities during penetration (Figure 4). It was found that the linear velocity of the bullet was decreased by each layer of the materials with different slopes showing the gradients between time and linear velocity. Therefore, as the degree of the negative slope in the specific material region became stronger,

the material was effective at decreasing the linear velocity rapidly. According to the regression of the first linear equation in each penetrating region, the cornstarch suspension showed a slightly larger degree of the negative slope than Hanji as given below:

$$\text{Linear Velocity (Hanji)} = -0.274t + 408.15 \quad (5)$$

$$\text{Linear Velocity (cornstarch suspension)} = -0.363t + 407.99 \quad (6)$$

where t is the time in μs during penetration. Therefore, compared to Hanji, the STF was effective in decreasing the linear velocity of the bullet. The linear velocity of the bullet in the initial FEA simulations was decreased by approximately 11% by the composite plate. On the other hand, the angular velocity was not affected by the composite plate. This was because the total penetration time was extremely short for the bullet to interact with the materials.

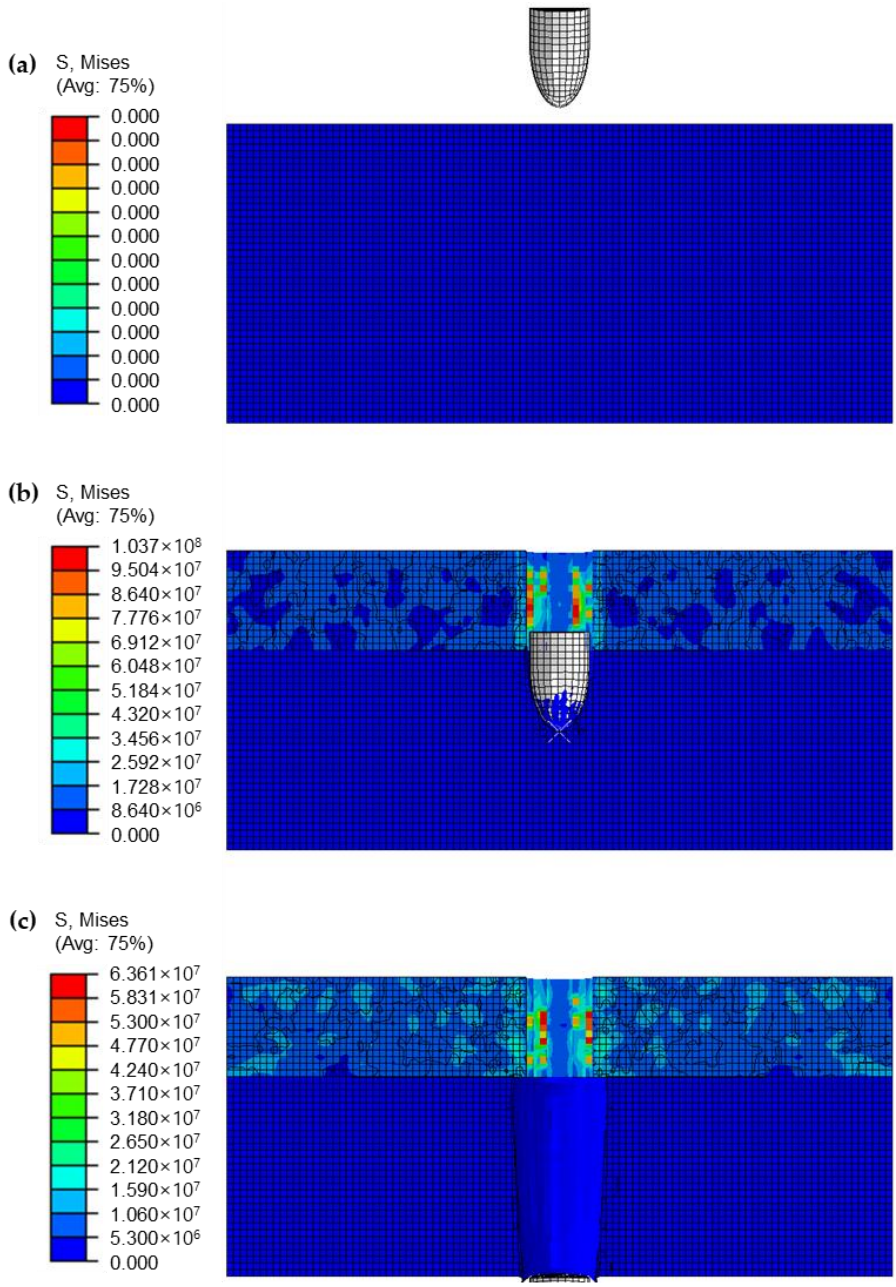

Figure 3. Equivalent stress calculated from simulation results using composites with 15-mm-thick Hanji and 30-mm-thick cornstarch layers suspension layers after (**a**) 0 μs, (**b**) 75 μs, and (**c**) 165 μs.

To identify the specific relationship between the thickness of each layer and the momentum of bullets, FEA was conducted by a set of central composite designs and changes of the linear velocity (Table 2). Then, the FEA results were evaluated using the second-order response surface regression as follows [31,32]:

$$V = -33.94 + 11.09x_1 + 23.08x_2 - 0.28x_1^2 - 0.37x_2^2 - 0.12x_1x_2, \quad (7)$$

where V is the linear velocity after penetration; and x_1 and x_2 are the thicknesses of Hanji and cornstarch suspension layers, respectively. In all the simulations, the angular velocity was not affected by the thickness of the materials. The response surface regression equation was partially differentiated to investigate the effect of each material on the linear velocity as shown below:

$$\frac{\partial V}{\partial x_1} = 11.10 - 0.56x_1 \quad (8)$$

$$\frac{\partial V}{\partial x_2} = 23.08 - 0.74x_2. \quad (9)$$

The cornstarch suspension was more effective at decreasing the linear velocity of bullets than Hanji. This tendency to influence the momentum of bullets can be attributed to strain hardening [33,34]. As the cornstarch suspension had much higher strain deformation than Hanji, its resistance to the impact gradually increased and thereby reduced the momentum of the bullet. Furthermore, it is reported that STFs can be solidified by transient hydroclustered particles in the STF momentarily under a high shear rate or under impact from a rod-like object [16–19]. Namely, the impact of the bullet can cause the cornstarch suspension to behave as if it is transitioning from a liquid to a solid state. This was the reason why the cornstarch suspension layer had a concave exit hole after bullet penetration (Figure 3c), which was different from that on the Hanji layer.

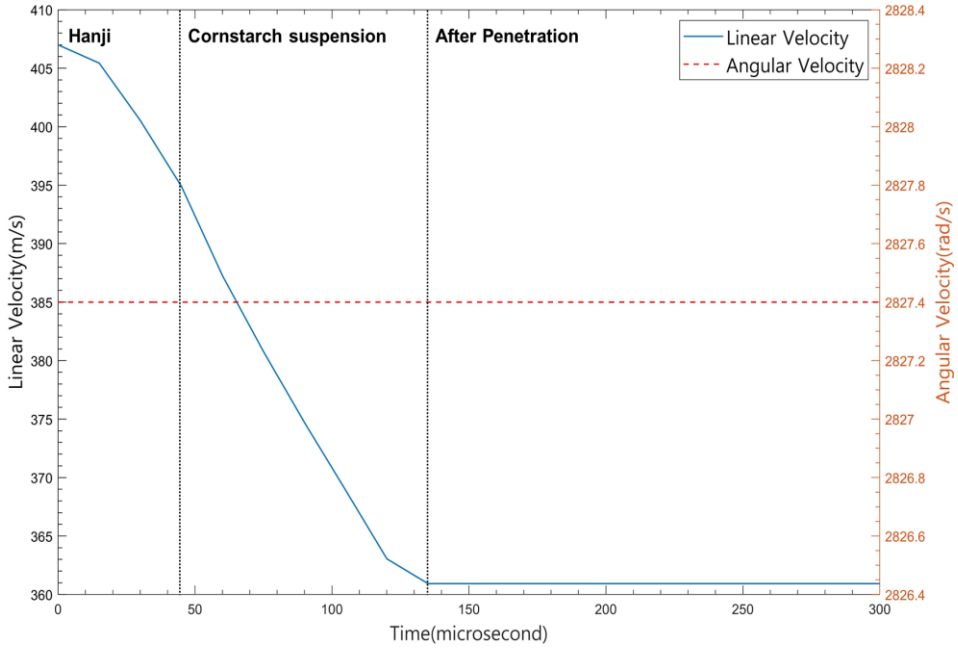

Figure 4. Changes in linear and angular velocities according to finite element analysis (FEA) in the composite plate with 15-mm-thick Hanji and 30-mm-thick cornstarch suspension layers over 300 μs.

Table 2. Linear velocity after penetration calculated from FEA conducted via central composite.

Hanji thickness (mm)	STF thickness (mm)	Linear Velocity (m/s)
20	35	351.167
20	25	361.294
15	37.07	353.632
22.07	30	354.282
15	30	360.928
15	22.93	367.92
7.93	30	367.304
10	35	360.435
10	25	370.684

3.3. Hole Diameters in the Witness Clay Pieces after Penetration

During bulletproof tests in the field, the cornstarch suspension showed outstanding resistance to bullet impact as the normalized perforated area decreased. Comparisons between the normalized perforated areas calculated in the experiments and simulations showed that as the thickness of the STF layers increased, the area of the witness clay penetrated by the bullet decreased owing to the decreasing momentum of the bullet (Figure 2b). However, the normalized perforated area increased with increases in the Hanji layer thickness, even though the linear velocity of the bullet was decreased in the Hanji region (Figure 2a). Thus, it was assumed that in addition to the momentum of the bullet, the impact stress also propagated through the composite plate, and it was eventually transferred to the clay piece. During penetration, Hanji had a much higher order of stress distribution over a broad region compared to that of the cornstarch suspension (Figures 5 and 6). It could be interpreted that the witness clay received a higher level of stress from the end of the Hanji layers. Based on the bullet momentum and impact stress propagation, the results of bulletproof performance tests conducted in the field and those of the additional FEA simulations were examined to evaluate the normalized perforated area. Ausiello et al. and several researchers calculated von Mises stress distribution in layered materials through FEM and utilized their calculations to analyze their own issues [35–37]. Under the same conditions used during FEA to analyze the momentum of bullet, nodes on the 40 mm × 40 mm region on the back side were selected as the medium for stress propagation to the clay (Figure S5). Until the time that the bullet penetrated the plate completely, the von Mises stresses on these nodes were added up. Therefore, the stress momentum generated by stress propagation and bullet momentum generated by the linear velocity at the specific time were calculated using the sum of the von Mises stresses at the nodes as follows:

$$M_{stress} = t_p \times A \times \sigma_{Tot} \tag{10}$$

$$M_{bullet} = m_{bullet} \times v_p \tag{11}$$

where t_p and v_p respectively represent the time and velocity of the bullet at complete penetration, σ_{Tot} is the total von Mises stress at the selected nodes until t_p, A is the area of selected nodes, and m_{bullet} is the mass of the bullet.

According to FEA results, the stress momentum in the Hanji layers was much higher, of the order of approximately ~ 10^7, than that of the cornstarch suspension having the same thickness (Figure 7a,b). Specifically, the stress momentum values of the Hanji layers (with thicknesses of 30, 45, and 60 mm) largely increased to 1155.0, 1947.7, and 3012.2 kg·m/s, respectively, while those of the cornstarch layers with the same thicknesses increased slightly to 0.9×10^{-3}, 1.3×10^{-3}, and 1.7×10^{-3} kg·m/s compared to the stress momentum values of the Hanji layers. Furthermore, the linear velocity of the bullet in the cornstarch suspension decreased considerably, resulting in a lower bullet momentum compared to that in Hanji (Figure 7c,d). The bullet momentum values in the Hanji layers (30, 45, and 60 mm) were 3.1917, 3.0684, and 2.9420 kg·m/s, respectively, while those in the cornstarch layers (with the same thicknesses) were respectively 3.1704, 3.0355, and 2.9068 kg·m/s. In this context, the stress

momentum effect on witness clay failure is negligible when penetrating the cornstarch suspension; thus, the bullet momentum was the dominant factor in witness clay failure, and the normalized perforated area decreased with decreasing bullet momentum (Figure 2b). On the contrary, the stress momentum in Hanji was much higher than the bullet momentum (Figure 7a,c); thus, we focused on the stress momentum when analyzing the witness clay failure. On increasing the thickness of the Hanji layer, the stress momentum continuously increased and could be transferred to the witness clay (Figure 7a). The perforated area on the witness clay increased with increases in the thickness of the Hanji layers owing to increases in the stress momentum. In summary, based on the perforated clay area of in-field tests, FEA assisted in analyzing how each Hanji and cornstarch suspension influenced the bullet and performed as the bulletproof layer. Despite the lack of mechanical properties considering high strain rate, FEA results were enough to indicate the bulletproof effect of materials with the results of perforated clay area through the momentum of bullet and stress propagation. Considering the clay piece as the protecting object being protected from the bullet, the STF (cornstarch) was very effective in decreasing the bullet momentum as well as the overall stress momentum. However, for ensuring the durability and stability of the armor itself, Hanji was the suitable material to absorb the stress resulting from the initial impact of the bullet. According to the National Institute of Justice 0101.06 of the U.S. Department of Justice, this study conducted the in-field bulletproof test similar with body armor classification of Type II [38]. There were no complete bulletproof plates to satisfy this classification. However, through the comparison between in-field tests and FEA simulations, it was enough to comprehend the bulletproof behaviors of Hanji and cornstarch suspension, which represent long fiber paper and STF, respectively, in a relative sense.

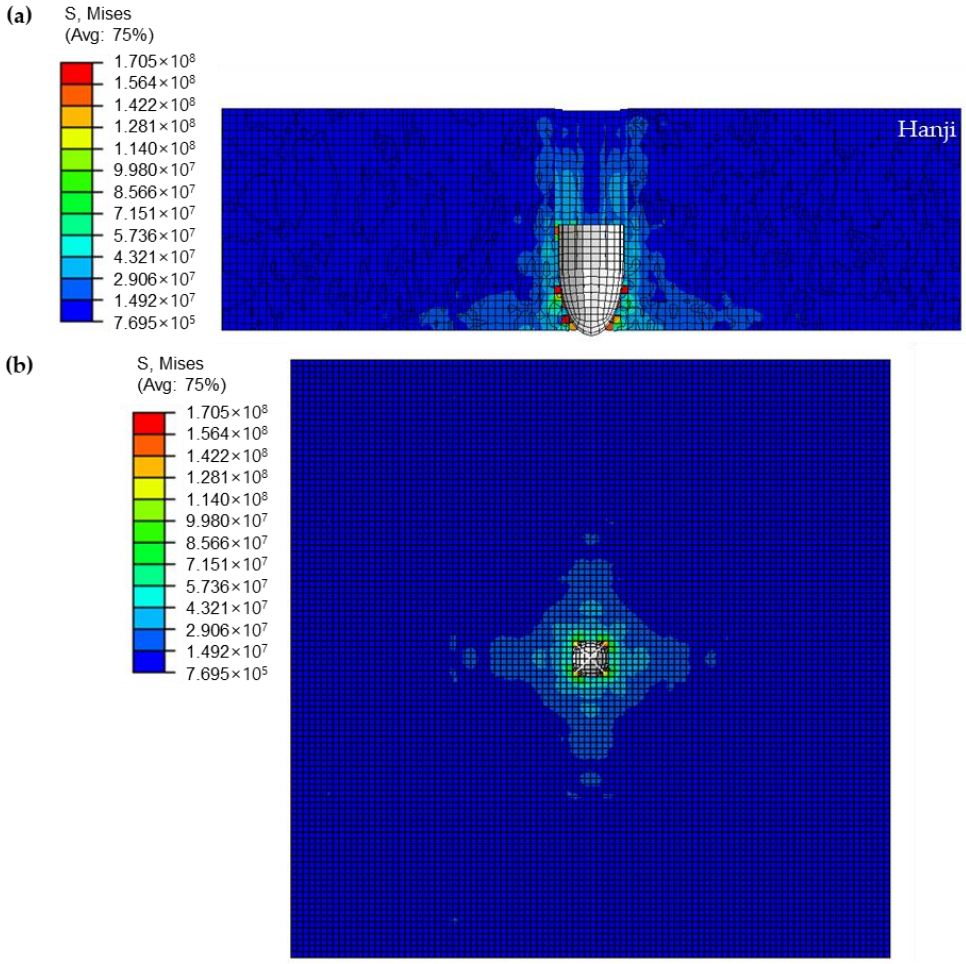

Figure 5. Stress distribution in 30-mm-thick Hanji at the instant of penetration as viewed from the (**a**) side and (**b**) bottom.

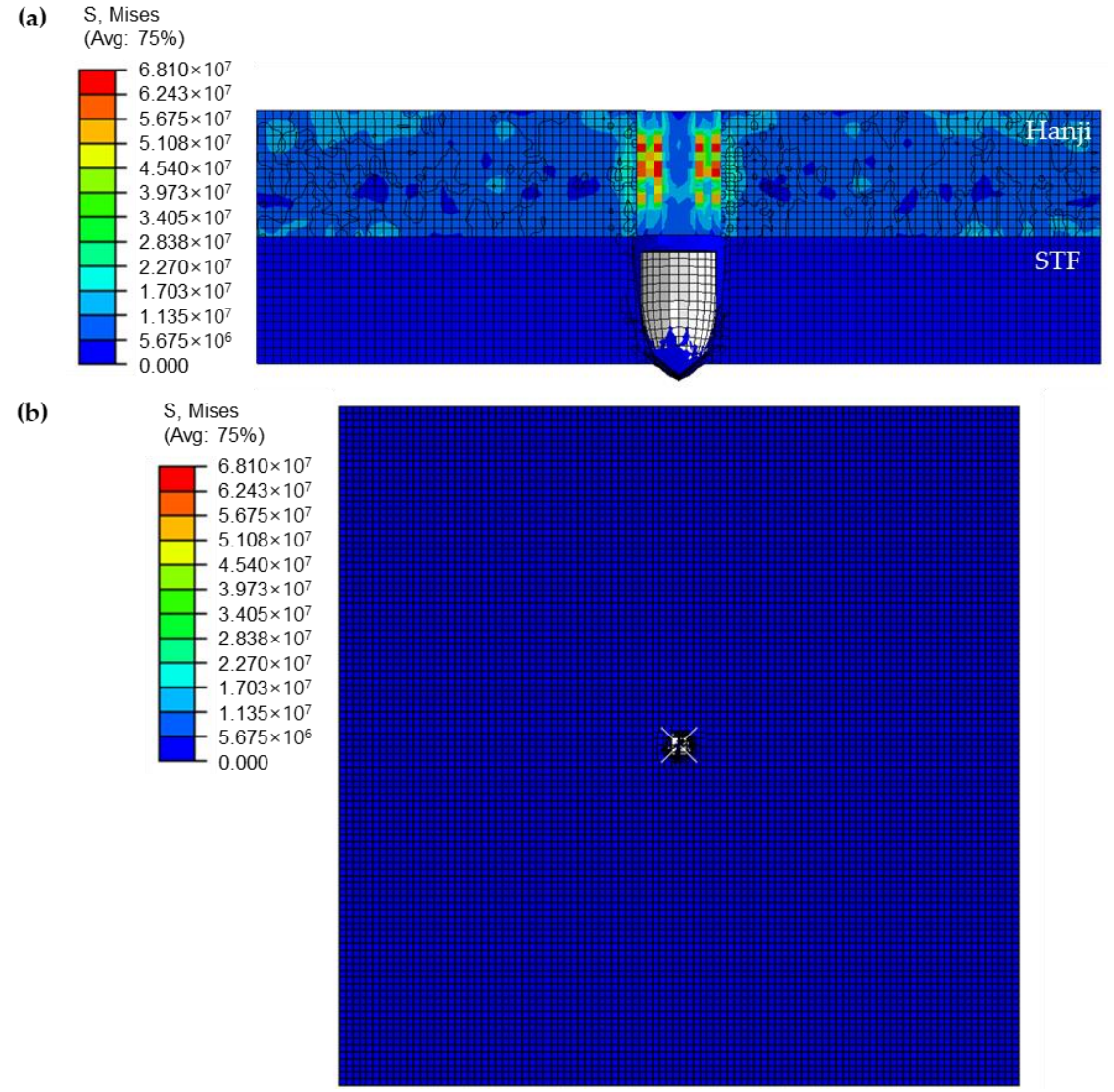

Figure 6. Stress distribution in the 15-mm-thick STF layer after passing through the 15-mm-thick Hanji layer at the instant of penetration in the (**a**) cross-section region and (**b**) bottom region.

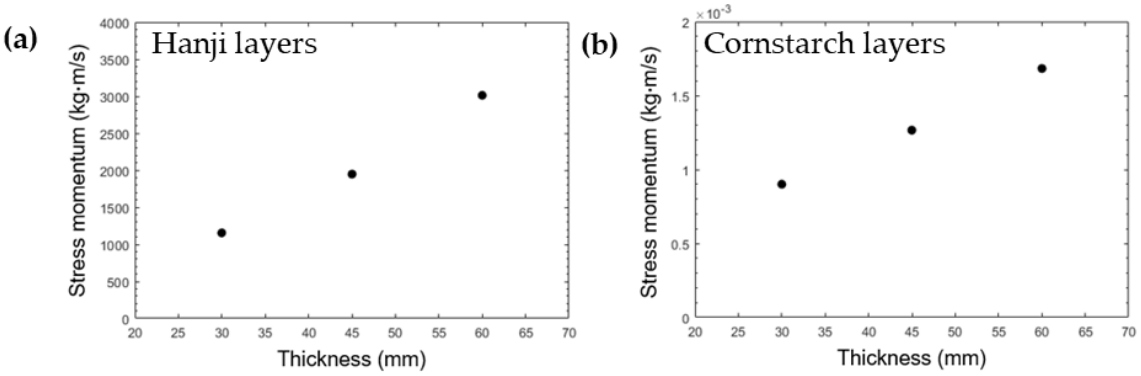

Figure 7. *Cont.*

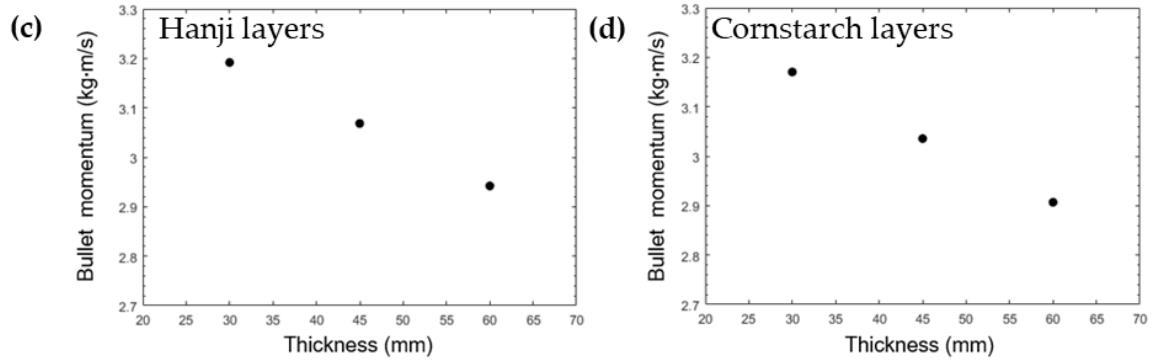

Figure 7. Stress momentum for various thicknesses of (**a**) Hanji layers and (**b**) cornstarch layers. Bullet momentum values calculated for various thicknesses of (**c**) Hanji layers and (**d**) cornstarch layers.

4. Conclusions

In this study, using the normalized perforated area, the bulletproof performance of eco-friendly Hanji–cornstarch biocomposites was analyzed with different numbers of Hanji layers and various thicknesses of cornstarch suspension layers. FEA simulations were conducted for analyzing the bulletproof performance of the Hanji and cornstarch layers. The results showed that the linear velocity of the bullet decreased with increases in the thicknesses of both the Hanji and cornstarch layers. The normalized perforated area of the Hanji–cornstarch composites decreased with increases in the thickness of the cornstarch layers, while it gradually increased when increasing the number of Hanji layers without cornstarch suspension layers. This is because the perforated area on the witness clay piece was mainly influenced by the stress momentum, which was propagated by the bullet impact on the bulletproof plate rather than the bullet momentum. The stress momentum increased with an increase in both the number of Hanji layers and the thickness of the cornstarch layers, but the stress momentum in the Hanji layers was a lot greater in comparison with the stress momentum in the cornstarch layers. We inferred that the bulletproof performance of Hanji–cornstarch composites was influenced significantly by the both bullet momentum and the stress momentum. Accordingly, we fabricated bulletproof biocomposites using cost-effective and easily fabrication process compared to previous papers using Kevlar. The findings of this work would be beneficial to the munitions industry owing to the facile and cost-effective manufacturing process used and favorable bulletproof performance of the Hanji–cornstarch biocomposites. Based on the results of this study, developing thin biocomposite-based bulletproof plates will be beneficial to enhance the mobility of armors as the future work.

Supplementary Materials: The following are available online at http://www.mdpi.com/2076-3417/10/1/88/s1, Figure S1. Fabrication of bulletproof composite plates using LbL method: (**a**) Assembling the Hanji layers by applying adhesive, (**b**) Cornstarch suspension stored in the zipper bag, and (**c**) composite plate formed by LbL of Hanji and applying cornstarch suspension, Figure S2 Comparison of (**a**) commercially available 9-mm bullet and (**b**) 9-mm bullet modeled in this study, Figure S3, Actual images obtained during bulletproof experiments for (**a**) composite with 20-mm-thick cornstarch suspension layers and 60 sheets of Hanji and (**b**) composite with no cornstarch layers and 120 Hanji layers, Figure S4. (**a**) Perforated diameter of clay after bulletproof experiments using composites with various Hanji layer sheets and (**b**) perforated diameter of clay after bulletproof experiments using hybrid composites composed of Hanji (60 sheets) and various thickness of cornstarch suspension (STF) layers, Figure S5. Nodes on the 40 mm ×40 mm region of the plate as viewed from the (**a**) side and (**b**) bottom, Table S1. Mechanical properties of Hanji and cornstarch suspension, Built-in function in ABAQUS/CAE

Author Contributions: Conceptualization, H.C., J.L., S.H., and S.K.; Experiments, H.C., J.L., and S.H.; Simulation, J.L.; Formal analysis, H.C. and J.L.; Investigation, H.C.; Writing-original draft, H.C., J.L., and S.H.; Writing-review, S.K.; Supervision, S.K. All authors have read and agreed to the published version of the manuscript.

Funding: This work was supported by the National Research Foundation of Korea (NRF) grant funded by the Korea government (MSIT) [grant number NRF-2018R1C1B6002339] and the Chung-Ang University Research Scholarship Grants in 2019.

Conflicts of Interest: The authors declare no conflict of interest.

References

1. Shim, G.I.; Kim, S.H.; Eom, H.W.; Ahn, D.L.; Park, J.K.; Choi, S.Y. Improvement in ballistic impact resistance of a transparent bulletproof material laminated with strengthened soda-lime silicate glass. *Compos. Part B Eng.* **2015**, *77*, 169. [CrossRef]
2. Monteiro, S.N.; Milanezi, T.L.; Louro, L.H.L.; Lima Jr, É.P.; Braga, F.O.; Gomes, A.V.; Drelich, J.W. Novel ballistic ramie fabric composite competing with Kevlar™ fabric in multilayered armor. *Mater. Des.* **2016**, *96*, 263. [CrossRef]
3. Forde, L.C.; Proud, W.G.; Walley, S.M.; Church, P.D.; Cullis, I.G. Ballistic impact studies of a borosilicate glass. *Int. J. Impact Eng.* **2010**, *37*, 568. [CrossRef]
4. Lee, Y.S.; Wetzel, E.D.; Wagner, N.J. The ballistic impact characteristics of Kevlar® woven fabrics impregnated with a colloidal shear thickening fluid. *J. Mater. Sci.* **2003**, *38*, 2825. [CrossRef]
5. Shim, G.I.; Kim, S.H.; Ahn, D.L.; Park, J.K.; Jin, D.H.; Chung, D.T.; Choi, S.Y. Experimental and numerical evaluation of transparent bulletproof material for enhanced impact-energy absorption using strengthened-glass/polymer composite. *Compos. Part B Eng.* **2016**, *97*, 150. [CrossRef]
6. Xie, W.; Tadepalli, S.; Park, S.H.; Kazemi-Moridani, A.; Jiang, Q.; Singamaneni, S.; Lee, J.H. Extreme mechanical behavior of nacre-mimetic graphene-oxide and silk nanocomposites. *Nano Lett.* **2018**, *18*, 987. [CrossRef]
7. Kim, S.; Xiong, R.; Tsukruk, V.V. Probing Flexural Properties of Cellulose Nanocrystal–Graphene Nanomembranes with Force Spectroscopy and Bulging Test. *Langmuir* **2016**, *32*, 5383. [CrossRef]
8. Raghavendra, G.M.; Jung, J.; Kim, D.; Seo, J. Effect of chitosan silver nanoparticle coating on functional properties of Korean traditional paper. *Prog. Org. Coat.* **2017**, *110*, 16. [CrossRef]
9. Jeong, M.J.; Bogolitsyna, A.; Jo, B.M.; Kang, K.Y.; Rosenau, T.; Potthast, A. Deterioration of ancient Korean paper (Hanji), treated with beeswax: A mechanistic study. *Carbohydr. Polym.* **2014**, *101*, 1249. [CrossRef]
10. Ko, Y.; Kwon, M.; Bae, W.K.; Lee, B.; Lee, S.W.; Cho, J. Flexible supercapacitor electrodes based on real metal-like cellulose papers. *Nat. Commun.* **2017**, *8*, 536. [CrossRef]
11. Choi, J.I.; Chung, Y.J.; Kang, D.I.; Lee, K.S.; Lee, J.W. Effect of radiation on disinfection and mechanical properties of Korean traditional paper, Hanji. *Radiat. Phys. Chem.* **2012**, *81*, 1051. [CrossRef]
12. Park, T.Y.; Lee, S.G. A study on coarse Hanji yarn manufacturing and properties of the Hanji fabric. *Fibers Polym.* **2013**, *14*, 311. [CrossRef]
13. Jeong, M.J.; Kang, K.Y.; Bacher, M.; Kim, H.J.; Jo, B.M.; Potthast, A. Deterioration of ancient cellulose paper, Hanji: Evaluation of paper permanence. *Cellulose* **2014**, *21*, 4621. [CrossRef]
14. Bender, J.W.; Wagner, N.J. Optical measurement of the contributions of colloidal forces to the rheology of concentrated suspensions. *J. Colloid Interface Sci.* **1995**, *172*, 171. [CrossRef]
15. Cheng, X.; McCoy, J.H.; Israelachvili, J.N.; Cohen, I. Imaging the microscopic structure of shear thinning and thickening colloidal suspensions. *Science* **2011**, *333*, 1276. [CrossRef]
16. Waitukaitis, S.R.; Jaeger, H.M. Impact-activated solidification of dense suspensions via dynamic jamming fronts. *Nature* **2012**, *487*, 205. [CrossRef]
17. Maranzano, B.J.; Wagner, N.J. Flow-small angle neutron scattering measurements of colloidal dispersion microstructure evolution through the shear thickening transition. *J. Chem. Phys.* **2002**, *117*, 10291. [CrossRef]
18. Farr, R.S.; Melrose, J.R.; Ball, R.C. Kinetic theory of jamming in hard-sphere startup flows. *Phys. Rev. E* **1997**, *55*, 7203. [CrossRef]
19. Melrose, J.R.; Van Vliet, J.H.; Ball, R.C. Continuous shear thickening and colloid surfaces. *Phys. Rev. Lett.* **1996**, *77*, 4660. [CrossRef]
20. Fall, A.; Huang, N.; Bertrand, F.; Ovarlez, G.; Bonn, D. Shear thickening of cornstarch suspensions as a reentrant jamming transition. *Phys. Rev. Lett.* **2008**, *100*, 018301. [CrossRef]
21. Brown, E.; Jaeger, H.M. Dynamic jamming point for shear thickening suspensions. *Phys. Rev. Lett.* **2009**, *103*, 086001. [CrossRef] [PubMed]
22. White, E.E.B.; Chellamuthu, M.; Rothstein, J.P. Extensional rheology of a shear-thickening cornstarch and water suspension. *Rheol. Acta* **2010**, *49*, 119. [CrossRef]
23. Cai, Z.; Li, Z.; Dong, J.; Mao, Z.; Wang, L.; Xian, C.J. A study on protective performance of bullet-proof helmet under impact loading. *J. Vibroeng.* **2016**, *18*, 2495.

24. Srivastava, A.; Majumdar, A.; Butola, B.S. Improving the impact resistance performance of Kevlar fabrics using silica based shear thickening fluid. *Mater. Sci. Eng. A* **2011**, *529*, 224–229. [CrossRef]
25. Marsyahyo, E.; Jamasri; Rochardjo, H.S.B.; Soekrisno. Preliminary investigation on bulletproof panels made from ramie fiber reinforced composites for NIJ level II, IIA, and IV. *J. Ind. Text.* **2009**, *39*, 13. [CrossRef]
26. Ning, H.; Li, J.; Hu, N.; Yan, C.; Liu, Y.; Wu, L.; Liu, F.; Zhang, J. Interlaminar mechanical properties of carbon fiber reinforced plastic laminates modified with graphene oxide interleaf. *Carbon* **2015**, *91*, 224. [CrossRef]
27. Kim, S.; Geryak, R.D.; Zhang, S.; Ma, R.; Calabrese, R.; Kaplan, D.L.; Tsukruk, V.V. Interfacial Shear Strength and Adhesive Behavior of Silk Ionomer Surfaces. *Biomacromolecules* **2017**, *18*, 2876. [CrossRef]
28. Fall, A.; Bertrand, F.; Hautemayou, D.; Mézière, C.; Moucheront, P.; Lemaitre, A.; Ovarlez, G. Macroscopic discontinuous shear thickening versus local shear jamming in cornstarch. *Phys. Rev. Lett.* **2015**, *114*, 098301. [CrossRef]
29. Fall, A.; Bertrand, F.; Ovarlez, G.; Bonn, D. Shear thickening of cornstarch suspensions. *J. Rheol.* **2012**, *56*, 575. [CrossRef]
30. Abaqus, V. 6.14 Documentation. *Dassault Syst. Simulia Corp.* **2014**, *651*, 23.1.1-8. Available online: http://130.149.89.49:2080/v6.14/pdf_books/ANALYSIS_3.pdf (accessed on 15 November 2019).
31. Liu, S.; Yang, F.; Zhang, C.; Ji, H.; Hong, P.; Deng, C. Optimization of process parameters for supercritical carbon dioxide extraction of Passiflora seed oil by response surface methodology. *J. Supercrit. Fluids* **2009**, *48*, 9. [CrossRef]
32. Nguyen, X.S.; Sellier, A.; Duprat, F.; Pons, G. Adaptive response surface method based on a double weighted regression technique. *Probabilistic Eng. Mech.* **2009**, *24*, 135. [CrossRef]
33. Forrestal, M.J.; Brar, N.S.; Luk, V.K. Penetration of strain-hardening targets with rigid spherical-nose rods. *J. Appl. Mech.* **1991**, *58*, 7. [CrossRef]
34. Warren, T.L.; Forrestal, M.J. Effects of strain hardening and strain-rate sensitivity on the penetration of aluminum targets with spherical-nosed rods. *Int. J. Solids Struct.* **1998**, *35*, 3737. [CrossRef]
35. Ausiello, P.; Apicella, A.; Davidson, C.L. Effect of adhesive layer properties on stress distribution in composite restorations—A 3D finite element analysis. *Dent. Mater.* **2002**, *18*, 295. [CrossRef]
36. Boschian Pest, L.; Guidotti, S.; Pietrabissa, R.; Gagliani, M. Stress distribution in a post-restored tooth using the three-dimensional finite element method. *J. Oral Rehabil.* **2006**, *33*, 690. [CrossRef]
37. Ranjbar-Far, M.; Absi, J.; Mariaux, G.; Dubois, F. Simulation of the effect of material properties and interface roughness on the stress distribution in thermal barrier coatings using finite element method. *Mater. Des.* **2010**, *31*, 772. [CrossRef]
38. Standard, N.I.J. *Ballistic Resistance of Body Armor NIJ Standard-0101.06*; US Department of Justice, Office of Justice Programs, National Institute of Justice: Washington, DC, USA, 2008.